Gas Hydrates of Argon and Methane Synthesized at High Pressures: Composition, Thermal Expansion, and Self-Preservation

Andrey G. Ogienko,[†] Alexander V. Kurnosov,[†] Andrey Y. Manakov,*[,†] Eduard G. Larionov,[†] Aleksei I. Ancharov,[‡] Mikhail A. Sheromov,[§] and Anatoly N. Nesterov[||]

Nikolaev Institute of Inorganic Chemistry SB RAS, Prospekt Akad. Lavrentieva 3, Novosibirsk, 630090, Russian Federation, Institute of Solid State Chemistry SB RAS, Kutateladze 18, Novosibirsk, 630128, Russian Federation, [3]Budker Institute of Nuclear Physics SB RAS, Prospekt Akad. Lavrentieva 11, Novosibirsk, 630090, Russian Federation, and Institute of Earth Cryosphere SB RAS, 86, Malygina str., Tyumen, 625026, Russian Federation

Received: July 16, 2005; In Final Form: November 14, 2005

For the first time, the compositions of argon and methane high-pressure gas hydrates have been directly determined. The studied samples of the gas hydrates were prepared under high-pressure conditions and quenched at 77 K. The composition of the argon hydrate (structure H, stable at 460−770 MPa) was found to be $Ar\cdot(3.27 \pm 0.17)H_2O$. This result shows a good agreement with the refinement of the argon hydrate structure using neutron powder diffraction data and helps to rationalize the evolution of hydrate structures in the Ar−H_2O system at high pressures. The quenched argon hydrate was found to dissociate in two steps. The first step (170−190 K) corresponds to a partial dissociation of the hydrate and the self-preservation of a residual part of the hydrate with an ice cover. Presumably, significant amounts of ice I*c* form at this stage. The second step (210−230 K) corresponds to the dissociation of the residual part of the hydrate. The composition of the methane hydrate (cubic structure I, stable up to 620 MPa) was found to be $CH_4\cdot5.76H_2O$. Temperature dependence of the unit cell parameters for both hydrates has been also studied. Calculated from these results, the thermal expansivities for the structure H argon hydrate are $\alpha_a = 76.6\ K^{-1}$ and $\alpha_c = 77.4\ K^{-1}$ (in the 100−250 K temperature range) and for the cubic structure I methane hydrate are $\alpha_a = 32.2\ K^{-1}$, $\alpha_a = 53.0\ K^{-1}$, and $\alpha_a = 73.5\ K^{-1}$ at 100, 150, and 200 K, respectively.

Introduction

The determination of precise gas hydrate composition is a complex experimental task due to difficulties in preparation of an ice-free hydrate sample and the prevention of gas release from the sample. Another problem arises from the nature of these compounds. As a rule, gas hydrates are nonstoichiometric compounds and their composition depends on the conditions of their synthesis and storage. For hydrates of cubic structures I (CS-I) and II (CS-II), most frequently occurring at moderate pressures (for details see refs 1 and 2), the occupancy of the large cavities of the structures by the guest molecule was determined to be close to 1, whereas the occupancy of the small cavities may vary between 0 and 1.[3] Currently, the task of accurate determination of the composition of the most abundant CS-I and CS-II gas hydrates, synthesized at moderate pressures, is solved. Perfectly good gas hydrate compositions can be obtained by preparative, diffraction, and spectroscopic methods (e.g., 4−7). The hydrates of hexagonal structure H (HS-III),[8,9] also occurring at moderate pressure, are less studied. It is known that the structure H hydrates with large organic guest molecules (methylcyclohexane, adamantane, and so on) cannot exist without partial filling of the small cavities with the molecules of an additional gas (methane, xenon, hydrogen sulfide, and so on).[1] X-ray diffraction studies indicated 81% occupancy of the small cavities in structure H for the methylcyclohexane + methane hydrate.[10]

Another source of nonstoichiometry of gas hydrates in the high-pressure region was revealed in a neutron diffraction study.[11] The authors showed that at about 100 MPa the large cavities of CS-II nitrogen hydrate can accommodate more than one guest molecule. According to a more detailed study,[12] the composition of the hydrate is $N_2\cdot6.37H_2O$ at 14.8 MPa and $N_2\cdot5.49H_2O$ at 100 MPa. As pressure increases from 14 to 100 MPa, the occupancy of the guest N_2 molecules rises from 0.85 to 0.96 and from 0.98 to 1.17 in small and large cavities, respectively, which implies the accommodation of more than one guest molecule in a large cavity. Other examples of a multiple filling of the large cavities by the guest molecules were found by our group in the course of a neutron diffraction study on high-pressure hydrates forming in an argon−water system.[13,14] The structure refinement of a CS-II hydrate, stable below 460 MPa, indicates an appreciable increase of argon content in large cavities as pressure grows. A phase transition observed for this hydrate at 460 MPa corresponds to the transformation of the CS-II hydrate to an H-type hydrate, with large E-cavities filled with five atoms of argon (Figure 1). Such a mode of the cavity filling has not been observed for clathrate hydrates before. The refinement of neutron powder diffraction data shows that two positions inside the large cavity have the occupancy of 1, while six other positions have the occupancy of 0.5. Each of the small cavities D and D′ is occupied by one atom of argon. From the unit cell formula $E\cdot2D\cdot3D'\cdot34H_2O$, the composition should be $Ar\cdot3.4D_2O$ (studies were run on deuterium hydrates). Another argon hydrate, with previously

* To whom correspondence should be addressed. Tel: (7-383) 339 13 46. Fax: (7-383) 330 94 89. E-mail: manakov@che.nsk.su.
[†] Nikolaev Institute of Inorganic Chemistry SB RAS.
[‡] Institute of Solid State Chemistry SB RAS.
[§] Budker Institute of Nuclear Physics SB RAS.
[||] Institute of Earth Cryosphere SB RAS.

10.1021/jp053915e CCC: $33.50
Published on Web 01/21/2006

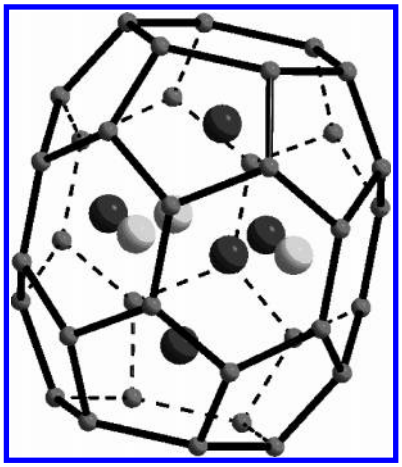

Figure 1. Positions of argon atoms in the large cavity of structure H.

unknown tetragonal structure, forms at pressures above 770 MPa.[14] The stoichiometry of this hydrate is $Ar \cdot 3D_2O$. The phase diagram of the methane−water system at pressures up to 1.5 GPa was studied in ref 15. At pressures up to 620 MPa, a methane hydrate of cubic structure I forms in the system. Another methane hydrate, of structure H, forms at higher pressures.[16] Large cavities of the latter hydrate are occupied by five methane molecules such as those for the argon hydrate mentioned above. Among experimentally measured characteristics of these hydrates, the composition obtained from the Rietveld refinement of powder X-ray data seems to be the most "doubtful". The doubts result from relatively small changes in the calculated diffraction pattern upon the variation of occupancy for guest positions as well as from the uncertainty of a thermal factor value for this atom. In addition, certain doubts on the possibility of accommodation of five argon atoms in a single large cavity were raised in a computation study.[17] Similar discrepancies exist for the composition of a hydrogen clathrate hydrate.[18,19] All this defined our interest in obtaining independent information on the composition of the high-pressure gas hydrates.

The quenching of the compounds prepared at high pressure (cooling in a high-pressure setup followed by a recovery of the frozen samples) is widely used. For example, a fair number of earlier investigations on the high-pressure modifications of ice were carried out using this method.[20] However, similar studies on gas hydrates were not reported. By the beginning of our studies, only one paper reported this sort of work, where the quenched samples of the high-pressure clathrate hydrate of tetrahydrofuran were produced.[21]

In this work, we present our data on the direct analytical determination of the compositions of high-pressure structure H argon and high-pressure cubic structure I methane gas hydrates as well as thermal expansion and self-preservation of these hydrates.

Experimental Section

The structure H argon hydrate was synthesized in a high-pressure piston-cylinder apparatus from thoroughly ground ice and an excess of gaseous argon at a pressure close to 760 MPa (the pressure of a diffraction experiment performed in ref 14). Methane hydrate was synthesized by the same method at a pressure of 500 MPa. To equilibrate the system, the mixture was kept at this pressure for 2−3 weeks. After that, the whole apparatus was cooled to 77 K in liquid nitrogen and a quenched sample of high-pressure hydrate was recovered. The sample was kept in liquid nitrogen no longer than 24 h before the measurements; no appreciable changes in the gas hydrate composition were observed within this period of time.

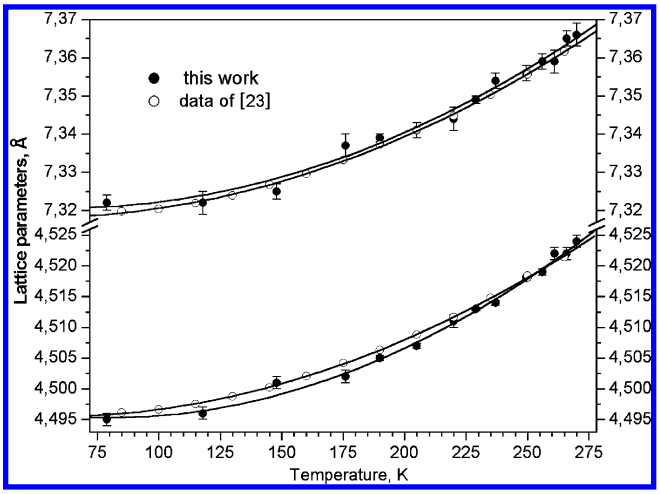

Figure 2. Comparison of lattice constants of ice I*h* between 79 and 270 K obtained in ref 23 and in this work.

Determination of the Composition of Hydrates. The release of gas from the studied samples was monitored as a function of temperature by collecting the gas into a calibrated buret placed into a concentrated aqueous NaCl solution. The weight of water remained after the decomposition of the hydrate was calculated as a difference of the cell weight before and after the experiment. The estimated size of the particles in the main fraction of the hydrate was about 0.1 mm. Three samples of the argon hydrate (each analyzed twice) and one sample of the methane hydrate were prepared. The weight of the hydrate samples used for the analyses was within 0.3−0.5 g. The measured gas volumes were corrected for vapor pressure other than the NaCl solution and were reduced to normal conditions. The composition of the hydrates was calculated from the measured quantities of gas and water. The accuracy of this method was verified by measuring the composition of a cubic structure II SF_6 hydrate prepared at 2 MPa (found hydrate number was 16.8 (8), from two independent determinations; the expected value is 17[1,3,4]). The maximal experimental error in our determinations was estimated to be ±6%.

Diffraction Experiment. X-ray diffraction studies were performed on quenched samples of the argon and methane hydrates and ice I*h* using synchrotron radiation at the fourth beamline of the VEPP-3 storage ring (Budker Institute of Nuclear Physics SB RAS), at fixed wavelength of 0.3675 Å.[22] The Debye−Sherrer scheme was applied. An imaging plate detector MAR3450 (pixel dimension 100 μm) was used to register the diffraction pattern. The distance between the sample and the detector calibrated against the diffraction pattern of sodium chloride was 391.0 mm. A fine-ground hydrate sample was placed in an aluminum cell with two foam-coated holes for the primary beam and the outlet of diffracted radiation. The cell was heated at the rate of about 3 °/min starting at 77 K. The diffraction patterns were recorded at various temperatures within 110−273 K.

Each diffraction pattern was collected for 4 min; the temperature value was taken as an average temperature in the course of a measurement. To verify the accuracy of the unit cell parameters determination, X-ray powder diffraction patterns of ice I*h* were recorded at various temperatures within 79−270 K. The comparison of the temperature dependences of the ice I*h* unit cell parameters derived in our experiments and those reported in ref 23 are presented in Figure 2. Good agreement

TABLE 1: Results of Experimental Determinations on the Composition ($Ar \cdot nH_2O$) of Quenched Argon Hydrate Synthesized at 760 MPa

hydrate number, *n*			
sample 1	sample 2	sample 3	average
3.50	3.14	3.20	3.27 ± 0.17
3.45	3.16	3.19	

between our results and the literature data prove the applicability of the experimental procedure utilized in this work.

Results and Discussion

Composition of Hydrates. Experimental data on the composition of a quenched high-pressure argon hydrate are listed in Table 1. Found stoichiometry $Ar \cdot (3.27 \pm 0.17)H_2O$ agrees, within experimental error, with the stoichiometry $Ar \cdot 3.4H_2O$ determined by the refinement of the hydrate structure.[14] The new data confirm the filling of the large cavity of the structure H hydrate by five argon atoms. In addition, our work demonstrates that the argon hydrate of structure H, stable at pressures 460−770 MPa, may be quenched and preserved; at 77 K, this hydrate can exist at least 24 h without appreciable decomposition. At atmospheric pressure, its dissociation becomes noticeable at 170 K. Complete decomposition of the structure H argon hydrate occurs between 170 and 230 K.

Our efforts to obtain quenched samples of the argon hydrate of tetragonal structure existing at pressures 770−920 MPa were not successful. The ejection of gas from the recovered samples occurred immediately after the pressure had been released at 77 K and the bulk hydrate solid transformed into a fine powder. The gas content in the powder was found to correspond to that of the argon hydrate of structure H that indicates the dissociation of the tetragonal structure argon hydrate into the structure H argon hydrate and gaseous argon.

The dissociation of the structure H argon hydrate proceeds in two steps; the gas release curves for the process are shown in Figure 3. Initially, it was assumed that the first step (170−190 K) corresponds to the transformation of the structure H hydrate to that of cubic structure II and the second step (210−230 K) to the dissociation of the cubic structure II hydrate. To verify this assumption, we recorded powder diffraction patterns for the quenched argon hydrate of structure H at 110−273 K (Figure 4). These results indicated that the argon hydrate of cubic structure II did not form but rather the structure H hydrate dissociated to hexagonal ice and gaseous argon. The most probable explanation for the "coexistence" of ice and the structure H argon hydrate is the self-preservation of the hydrate by an ice cover formed on the surface of the bulk hydrate sample. The structure H argon hydrate is less stable at ambient pressure than the cubic structure II argon hydrate; the latter dissociates at 149 K.[1] Nevertheless, the quenched sample of the structure H hydrate started to dissociate only above 170 K and existed up to 230 K. Apparently, below 170 K, the dissociation is inhibited by low temperature (quenching effect), while at 170−230 K, the dissociation is inhibited due to the self-preservation effect. The first step of the dissociation process, starting at about 170 K, stops due to the self-preservation of the residual part of the hydrate by an ice cover forming in the dissociation process and the process slows down dramatically. After heating to 220 K, the dissociation of the residual part of the hydrate occurs. The results of diffraction studies will be discussed further in the text.

In addition, the composition of cubic structure I methane hydrate prepared at a pressure of 500 MPa was determined by the same method (Figure 3). The dissociation of the methane hydrate proceeded in one step, and no self-preservation was observed provided that powdered methane hydrate was taken for the experiment. The composition of the studied sample was found to be $CH_4 \cdot 5.76H_2O$. The methane content in the hydrate slightly exceeded the previously reported methane content for the cubic structure I methane hydrate synthesized at a lower pressure ($CH_4 \cdot 6.0H_2O$[1,24,25]). The composition derived in this study corresponds to 100% occupation of both types of cavities in the cubic structure I hydrate framework, with each cavity being occupied by one methane molecule. Our experimental results show that the entry of more than one methane molecule into the large cavity of cubic structure I is impossible, presumably because of the considerable distortions of the hydrate framework this process would require.

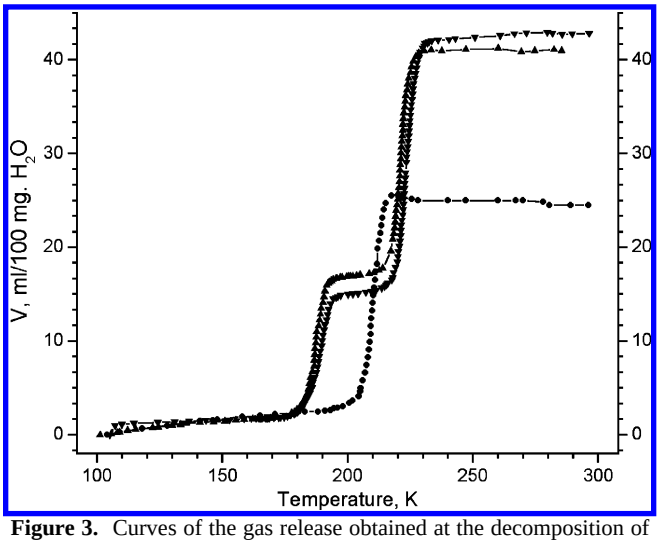

Figure 3. Curves of the gas release obtained at the decomposition of argon and methane hydrates (▲, argon hydrate; ●, methane hydrate).

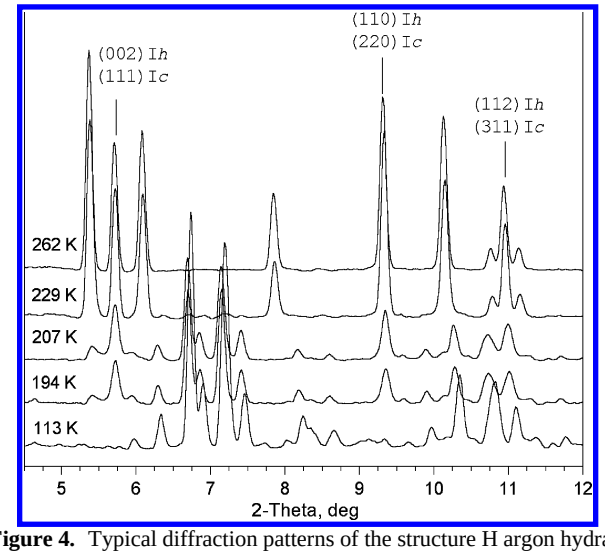

Figure 4. Typical diffraction patterns of the structure H argon hydrate at different temperatures.

Powder Diffraction: Dissociation of Hydrates and Thermal Expansion. Typical diffraction patterns of the samples of quenched structure H argon and cubic structure I methane hydrates, recorded at various temperatures, are presented in Figures 4 and 5. The temperature dependences of the lattice parameters for these hydrates, as well as for ice obtained in the course of the dissociation of the hydrates, are shown in Figures 6−8. In the case of the argon hydrate, the first reflections of hexagonal ice appear at about 180−190 K which corresponds to the temperature of the first step on the gas release curves. At

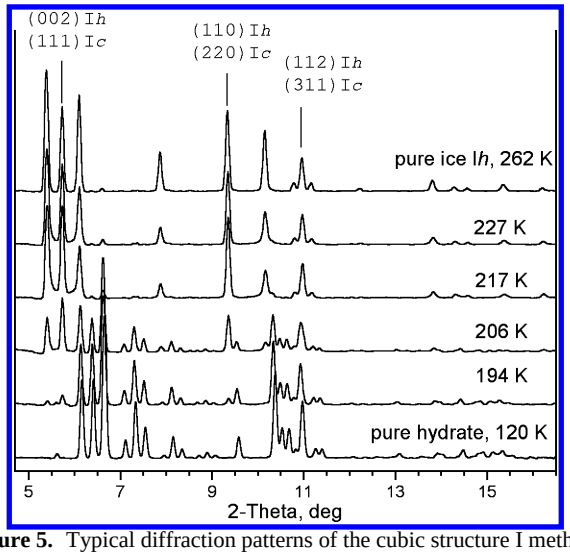

Figure 5. Typical diffraction patterns of the cubic structure I methane hydrate at different temperatures.

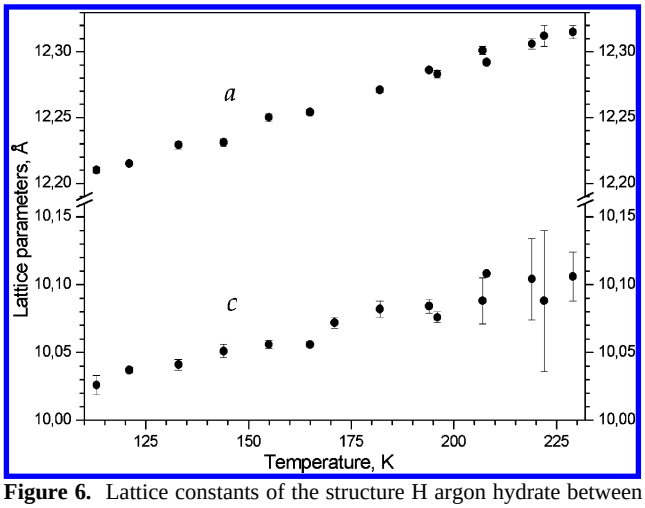

Figure 6. Lattice constants of the structure H argon hydrate between 110 and 240 K (the error bars for the *a* axis are smaller than the symbols themselves).

190−230 K, the diffraction pattern corresponds to a mixture of ice and hydrate, and above 230 K, only the reflections of ice I*h* are observed. The latter temperature corresponds to the end of the second step of the gas release.

The dissociation of methane hydrate occurred in a similar way. Below 210 K, powder diffraction patterns were consistent with those of the pure hydrate of cubic structure I. When powdery hydrate samples were used in the studies, the dissociation appeared as a sharp one-step process on the gas release curves (Figure 3). The diffraction patterns recorded after heating the samples above 210 K showed only reflections of pure ice I*h*. When small clots of stuck hydrate particles were used in the experiments, some amount of admixed methane hydrate was observed in the sample between 210 and 270 K indicating the self-preservation of the hydrate.

The variation of unit cell parameters for the structure H argon hydrate in the temperature range 113−229 K and for the cubic structure I methane hydrate in the temperature range 86−267 K may be described by the following relationships (the values in brackets show standard deviations expressed in the units of the last one or more digits)

$$a = 12.102(3) + 9.38(21) \times 10^{-4}T$$

$$c = 9.937(11) + 7.78(64) \times 10^{-4}T \text{ (structure H argon hydrate)}$$

$$a = 11.835(11) - 1.12(116) \times 10^{-4}T + 2.47(56) \times 10^{-6}T^2 \text{ (cubic structure I methane hydrate)}$$

The temperature dependence data for the unit cell parameters of ice I*h* (temperature range 79−270 K) were approximated by the following equations (Figure 2)

$$a = 4.500(3) - 1.23(27) \times 10^{-4}T + 7.76(70) \times 10^{-7}T^2$$

$$c = 7.324(5) - 1.24(56) \times 10^{-4}T + 1.02(53) \times 10^{-6}T^2$$

From these dependences, the thermal expansivities of the two hydrates were calculated using the equation $\alpha = 1/a_0(da/dT)$ (Table 2). The thermal expansivities of ice I*h* were calculated by two methods previously applied by others:[23,26−35] (1) relative to the unit cell parameters of ice at 263 K ($a_0 = 4.523$ Å, $c_0 = 7.367$ Å[26]) and (2) relative to the corresponding parameter at a given temperature. It is seen from Table 2 that the thermal expansivities calculated by the two methods are quite similar and are comparable to the corresponding values reported previously. The thermal expansivities of argon and methane hydrates were calculated by the second method.

The comparison of obtained thermal expansivities for the studied hydrates with those for hexamethylethane + Xe and 2,2-dimethylbutane + Xe[30] hydrates (isostructural with the argon hydrate) and for methane hydrate[31,33] (Table 2) shows a close agreement of the obtained values with the literature data for corresponding temperature intervals. There is a remarkable agreement between the values for the quenched high-pressure argon hydrate of structure H with unusual filling of the large cavity (five argon atoms) and the corresponding values for some other hydrates (Table 2). The invariation of the thermal expansivity for the argon hydrate as the temperature decreases indicates its essential dissimilarity from other hydrates for which a decrease in thermal expansivity at low temperatures was observed. As it was reported previously,[29] at low temperatures, the thermal expansion depends mainly on the interaction of guest molecules with the host framework, while at higher temperatures, it is determined by the vibrations of water molecules resulting in thermal expansivities similar to those of ice. Possibly, the peculiarities of the argon guest subsystem become apparent only at low temperatures. As mentioned above, the values of thermal expansivity for methane hydrate correspond well to the literature data. At the same time, found in this study, unit cell parameters are significantly different from the data of ref 31 but consistent with the results of ref 33 for methane deuteriohydrate (Figure 7). We believe that our results and the results of ref 33 are more precise because in each our experiment the diffraction patterns of ice I*h* were recorded in the process of hydrate dissociation and the reflections of ice were used as an internal standard (Figure 8). At temperatures 250−270 K, the deviations of our results from the standard literature values do not exceed 0.006 Å; the value might be taken as an estimation of the upper limit systematic experimental error. More significant differences observed at lower temperatures can be a result of imperfections in the ice structure formed in the hydrate dissociation process. Despite structural differences among different types of clathrate hydrates, all hydrates show greater expansivity than ice I*h*. This property may be a common feature inherent in all clathrate hydrates.

Powder Diffraction: Self-Preservation. As it was mentioned in the previous sections, we managed to obtain a set of X-ray diffraction patterns at different temperatures for the

TABLE 2: Coefficients of Thermal Expansion ($\times 10^6$) for Some Clathrate Hydrates and Ice[a]

			T, K			
			100	150	200	250
pure ice I*h*	α_a	this work	7.1 (7.2)	24.3 (24.4)	41.4 (41.6)	58.6 (58.6)
		23	11.9 (12.0)	25.0 (25.1)	38.1 (38.2)	51.2 (51.2)
	α_c	this work	10.8 (10.9)	24.7 (24.8)	38.5 (38.7)	52.4 (52.4)
		23	12.9 (13.0)	25.5 (25.7)	38.2 (38.3)	50.8 (50.9)
str. H Ar hydrate	α_a	this work		76.6		
	α_c	this work		77.4		
CS-I CH_4 hydrate	α_a	this work	32.2	53.0	73.5	
CS- I CH_4 hydrate	α_a	31	34.7	49.6	64.5	79.2
CS-I CO_2 hydrate	α_a	34	48.8	60.9	62.5	
air hydrate	α_a	32			44 (±9)	
CS-II THFD hydrate	α_a	35	28.1 (4)	44.4 (6)		77.0 (1.5)
CS-I EO hydrate	α_a	29	40	58	77	
str. H HME hydrate	α_a	30		60	78	
	α_c	30		24	71	
str. H DMB hydrate	α_a	30		54	67	
	α_c	30		40	59	

[a] Values of thermal expansivities given in parentheses were calculated by method 2 (see text). Maximum errors in the values of thermal expansivities obtained in this work are less than 5%. THFD, tetrahydrofuran d_8; EO, ethylene oxide; HME, hexamethylethane; DMB, 2,2-dimethylbutane.

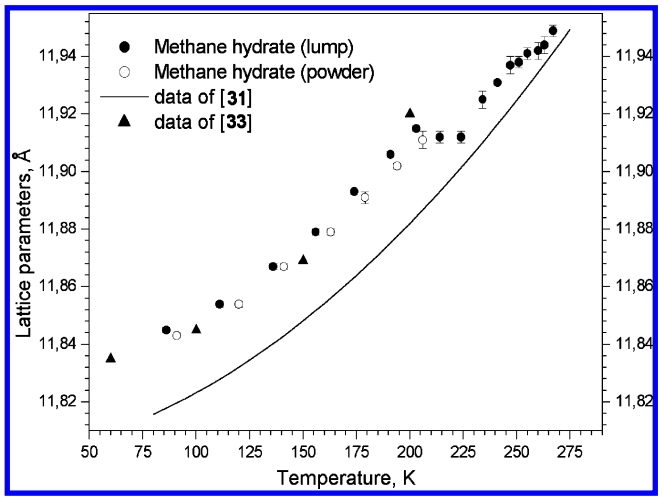

Figure 7. Lattice constant of the cubic structure I methane hydrate between 86 and 267 K.

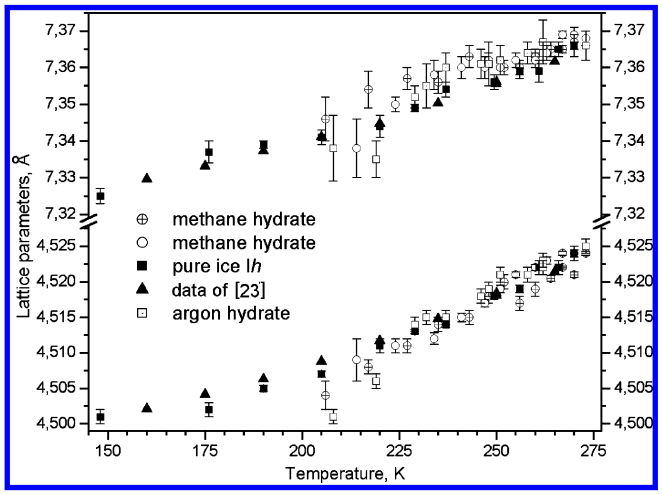

Figure 8. Comparison of *a* (bottom) and *c* (top) lattice constants of pure ice I*h* with the lattice parameters of ice I*h* obtained after decomposition of gas hydrates.

quenched samples of argon (structure H) and methane (cubic structure I) hydrates in both pure and ice-preserved states. In view of the fact that the self-preservation phenomenon is studied poorly, these data are worthy of more detailed consideration. In the case of the structure H argon hydrate, at the temperature corresponding to the first step of gas release, the appearance of ice I*h* reflections occurs nonuniformly. For example, upon the initial stages of the process, a primary growth of the ice I*h* 002 reflection was observed (as compared to 100 and 101 reflections). The intensity changes of these reflections in the temperature range 194−262 K are presented in Figures 4 and 5. Similar observations were reported for the methane hydrate,[36] but for the argon hydrate, the primary growth of the 002 reflection is more pronounced. The explanation of the nonuniform increase in intensity of the reflections of ice suggested in ref 36 is related to defects in the crystal structure of ice I*h* forming in the process. Another possibility is a simultaneous formation of ice I*h* and I*c* during the structure H argon hydrate dissociation. It is known that all reflections of ice I*c* are overlapped with the reflections of ice I*h*. At the same time, it is seen from Figures 4 and 5 that at the initial stage of the hydrate dissociation process a primary rise of the reflections overlapping with those of ice I*c* occurs. This observation allows us to suggest that, at temperatures lower than 230−240 K, ice I*c* is a major product of the hydrate dissociation that converts to ice I*h* at higher temperature. This conclusion explains significant deviations of the ice I*h* unit cell parameters from expected values in the temperature range 200−240 K (Figure 8) caused by a sharp rise in the experimental error. The error may arise from the simultaneous presence in the sample of both ice I*h* and ice I*c* phases that give overlapping reflections. Similar observations were made in the dissociation process of methane hydrate (Figure 5). It should be noted that, in addition to the anomalous behavior exhibited by ice, slightly pronounced features were found on the temperature dependencies of the hydrates unit cell parameters (Figures 6 and 7). In the region of self-preservation, the unit cells of methane and argon hydrates expand somewhat less than could be expected from the extrapolation of the other part of the curve. Additional studies would be recommended to investigate this effect in more detail.

The self-preservation phenomenon observed before for methane[37,38] and some other hydrates[39] is a drastic inhibition of hydrate dissociation caused by the formation of an ice crust on the surface of hydrate particles. It was found that self-preserved massive hydrate samples can exist for several months without any noticeable loss of gas. Some fractions of millimeter-sized hydrate particles exist for several hours at temperatures that are higher than the decomposition temperature of the hydrate.[40] According to ref 41, the minimal size of a hydrate particle which

may display the self-preservation phenomenon is a quarter of millimeter. As shown in ref 39, the self-preservation phenomenon occurs only in the temperature range 240−270 K. The observations presented in refs 36 and 42 indicate a distinction between the morphology of the ice cover on the surface of hydrate particles when the temperature ranges from 193 to 210 K and when the temperature exceeds 230 K. Individual particles close in size and shape are observed in the former case whereas an ice crust is observed in the latter. At present, no conventional explanation of the origin of the phenomenon is available.

It should be noted that for the decomposition reaction $A_{solid} \rightarrow B_{solid}$ + gas the inhibition of dissociation by a solid crust is well-known[43] and is believed to result from slow diffusion of the gas through a layer of the solid product. Such a mechanism was assumed for the methane hydrate.[40]

According to another model, the gas pressure is built up under the hydrate crust stabilizing the hydrate.[44] In this model, the hydrate crust is supposed to be absolutely impermeable, whereas in the model mentioned above the impermeability is only partial. The pressure model does not explain the preservation of ice by hydrates, the phenomenon related to that of the self-preservation of hydrates. One more interpretation of the phenomenon, taking into account both models, is given in ref 45. This explanation presumes an overheating of the preserved solid (hydrate) that is possibly due to the existence of a potential barrier generated by the ice crust. The crust prevents the nucleation of new phases making the realization of a surface fusion mechanism impossible under these conditions. Summarizing the above discussion, it is possible to conclude that no unequivocal explanation of the self-preservation phenomenon exists today. The comparison of our data and literature data does not reveal new information about the reasons for the hydrate self-preservation but makes it possible to speculate on the mechanism of the ice crust formation. As it was mentioned above, our data indicate the formation of ice I*c* during the hydrate dissociation at 230−240 K, while at higher temperatures the diffraction patterns reveal the formation of ice I*h*. The above temperature range corresponds to that of the homogeneous nucleation of water[46] (a minimal temperature to which liquid water can be overcooled) and to the transition temperature of a metastable ice modification, ice I*c*, into the stable ice I*h*.[36] When the fact that liquid water forms as an intermediate phase during the dissociation of gas hydrates to gas and ice[47,48] (according to the authors of ref 47, the first observation of this phenomenon was performed by Prof. Yu. F. Makogon in 60 s) is taken into account, it may be assumed that a change in the mechanism of methane hydrate self-preservation, observed at 230−240 K, is solely associated with the change in the mode of water crystallization. At low temperature, the produced water freezes immediately to form single uniformly sized crystals (also, a direct hydrate to solid ice transition is possible). At higher temperature, the water, produced during the hydrate dissociation, forms a thin film on the hydrate surface and rapidly freezes generating an ice shell. This mechanism explains the formation of an impermeable for gas ice crust on the hydrate surface. It should be noted that a visual observation of rapidly freezing water during the hydrate dissociation may not be simple.

The self-preservation of the structure H argon hydrate is observed in a temperature region where the probability of self-preservation for the methane hydrate is low. As shown in our diffraction experiments, the formation of ice I*c* plays a more prominent role in the self-preservation of the argon hydrate as compared to the methane hydrate. The dissociation of the self-preserved hydrate at 220−230 K coincides with the disappearance of ice I*c* in the system which, according to the diffraction studies, transforms into ice I*h* (Figure 4). The discussed observations disclose different mechanisms of self-preservation for the studied hydrates. Further studies are necessary to elucidate the mechanism of the formation of protecting ice crust on the surface of the structure H argon hydrate.

Conclusions

The present study compares the composition and properties of argon hydrate (structure H) and methane hydrate (cubic structure I) prepared at high pressures. It is shown for the first time that high-pressure gas hydrates could be quenched and subsequently studied at atmospheric pressure. It has been shown, using the structure H argon hydrate as an example, that the self-preservation phenomenon can be observed for high-pressure gas hydrates.

The study of diffraction patterns of the two hydrates at various temperatures reveals the appearance at about 200 K of noticeable amounts of ice I*c*. The studied thermal expansion curves were found to be close to those of other gas hydrates.

Acknowledgment. This work was supported by a grant of Presidium SB RAS No. 147. A.Y.M. thanks the "Russian Science Support Foundation" for financial support. Authors thanks Dr. A. Likhacheva for help in diffraction experiments.

References and Notes

(1) Sloan, E. D., Jr. *Clathrate Hydrates of Natural Gases*; 2nd Ed.; Marcel Dekker: New York, 1997.
(2) Jeffrey, G. A. Hydrate inclusion compounds. In *Comprehensive Supramolecular Chemistry*; Atwood, J. L., Davies, J. E. D., MacNicol, D. D., Vogtle, F., Eds.; Elsevier Science Ltd.: Oxford, U.K., 1996; Vol. 6. Solid-state supramolecular chemistry: Crystal engineering, p 757.
(3) Dyadin, Y. A. *Supramol. Chem.* **1995**, *6*, 59.
(4) Cady, G. H. *J. Phys. Chem.* **1981**, *85*, 3225.
(5) Ripmeester, J. A.; Ratcliffe, C. I. *J. Phys. Chem.* **1988**, *92*, 337.
(6) Sum, A. K.; Burruss, R. C.; Sloan, E. D., Jr. *J. Phys. Chem. B* **1997**, *101*, 7371.
(7) Udachin, K. A.; Enright, G. D.; Ratcliffe, C. I.; Ripmeester, J. A. *J. Am. Chem. Soc.* **1997**, *119*, 11481.
(8) Ripmeester, J. A.; Tse, J. S.; Ratcliffe, C. I.; Powell B. M. *Nature* **1987**, *325* (6100), 135.
(9) Udachin, K. A.; Ratcliffe, C. I.; Enright, G. D.; Ripmeester, J. A. *Supramol Chem.* **1997**, *8*, 173.
(10) Udachin, K. A.; Ratcliffe, C. I.; Ripmeester, J. A. *J. Supramol. Chem.* **2002**, *2*, 405.
(11) Kuhs, W. F.; Chazallon, B.; Radaelli P. G.; Pauer F. *J. Inclusion Phenom.* **1997**, *29*, 65.
(12) Chazallon, B.; Kuhs, W. F. *J. Chem. Phys.* **2002**, *117* (1), 308.
(13) Kurnosov, A. V.; Manakov, A. Y.; Komarov, V. Y.; Voronin, V. I.; Teplych, A. E.; Dyadin, Y. A. *Dokl. Phys. Chem.* **2001**, *381* (4−6), 649.
(14) Manakov, A. Y.; Voronin, V. I.; Kurnosov, A. V.; Teplych, A. E.; Komarov, V. Y.; Dyadin, Y. A. *J. Inclusion Phenom.* **2004**, *48*, 11.
(15) Dyadin, Y. A.; Aladko, E. Y.; Larionov, E. G. *Mendeleev Commun.* **1997**, 34.
(16) Loveday, J. S.; Nelmes, R. J.; Klug, D. D.; Tse, J. S.; Desgreniers, S. *Can. J. Phys.* **2003**, *81*, 539.
(17) Inerbaev, T. M.; Belosludov, V. R.; Belosludov, R. V.; Sluiter, M.; Kawazoe, Y.; Kudon, J.-I. *J. Inclusion Phenom.* **2004**, *48*, 55.
(18) Lokshin, K. A.; Zhao, Y.; He, D.; Mao, W. L.; Mao, H.-K.; Hemley, R. J.; Lobanov, M. V.; Greenblatt, M. *Phys. Rev. Lett.* **2004**, *93* (12), 125503 1−4.
(19) Mao, W. L.; Mao, H.-K.; Goncharov, A. F.; Struzhkin, V. V.; Guo, Q.; Hu, J.; Shu, J.; Hemley, R. J.; Somayazulu, M.; Zhao, Y. *Science* **2002**, *297*, 2247.
(20) Engelhardt, H.; Kamb, B. *J. Chem. Phys.* **1981**, *75* (12), 5887.
(21) Zakrzewski, M.; Klug, D. D.; Ripmeester, J. A. *J. Inclusion Phenom.* **1994**, *17*, 237.
(22) Ancharov, A. I.; Manakov, A. Y.; Mezentsev, N. A.; Tolochko, B. P.; Sheromov, M. A.; Tsukanov, V. M. *Nucl. Instrum. Methods Phys. Res., Sect. A* **2001**, *470*, 80.
(23) Rottger, K.; Endriss, A.; Ihringer, J.; Doyle, S.; Kuhs, W. F. *Acta Crystallogr. B* **1994**, *50*, 644.
(24) Handa, Y. P. *J. Chem. Thermodyn.* **1986**, *18*, 915

(25) Circone, S.; Kirby, S. H.; Stern, L. A. *J. Phys. Chem. B* **2005**, *109*, 9468.
(26) LaPlaca, S.; Post, B. *Acta Crystallogr.* **1960**, *13*, 503.
(27) Brill, v. R.; Tippe, A. *Acta Crystallogr.* **1967**, *23*, 343.
(28) Davidson, D. W.; Handa, Y. P.; Ratcliffe, C. I.; Ripmeester, J. A.; Tse, J. S.; Dahn, J. R.; Lee, F.; Calvert, L. D. *Mol. Cryst. Liq. Cryst.* **1986**, *141*, 141.
(29) Tse, J. S.; McKinnon, W. R.; Marchi, M. *J. Phys. Chem.* **1987**, *91*, 4188.
(30) Tse, J. S. *J. Inclusion Phenom.* **1990**, *8*, 25.
(31) Shpakov, V. P.; Tse, J. S.; Tulk, C. A.; Kvamme, B.; Belosludov, V. R. *Chem. Phys. Lett.* **1998**, *282*, 107.
(32) Takeya, S.; Nagaya, H.; Matsuyama, T.; Hondoh, T.; Lipenkov, V. Ya. *J. Phys. Chem. B* **2000**, *104*, 668.
(33) Gutt, C.; Asmussen, B.; Press, W.; Johnson, M. R.; Handa, Y. P.; Tse, J. S. *J. Chem. Phys.* **2000**, *113* (11), 4713.
(34) Udachin, K. A.; Ratcliffe, C. I.; Ripmeester, J. A. *J. Phys. Chem. B* **2001**, *105*, 4200.
(35) Jones, C. Y.; Marshall, S. L.; Chakoumakos, B. C.; Rawn, C. J.; Ishii, Y. *J. Phys. Chem. B* **2003**, *107*, 6026.
(36) Kuhs, W. F.; Genov, G.; Staykova, D. K.; Hansen, T. *Phys. Chem. Chem. Phys.* **2004**, *6*, 4917.
(37) Handa, Y. P. *J. Chem. Thermodyn.* **1986**, *18*, 891.
(38) Yakushev, V. S.; Istomin, V. AA. In *Physics and Chemistry of Ice*; Maeno, N., Hondoh, T., Eds.; Hokkaido University Press: Sapporo, Japan, 1992; p 136.
(39) Stern, L. A.; Circone, S.; Kirby, S. H.; Durham, W. B. *J. Phys. Chem. B* **2001**, *105*, 1756.
(40) Takeya, S.; Shimada, W.; Kamata, Y.; Ebinuma, T.; Uchida, T.; Nagao, J.; Narita, H. *J. Phys. Chem. A* **2001**, *105*, 9756.
(41) Takeya, S.; Uchida, T.; Nagao, J.; Ohmura, R.; Shimada, W.; Kamata, Y.; Ebinuma, T.; Narita, H. *Chem. Eng. Sci.* **2005**, *60*, 1383.
(42) Shimada, W.; Takeya, S.; Kamata, Y.; Uchida, T.; Nagao, J.; Ebinuma, T.; Narita, H. *J. Phys. Chem. B* **2005**, *109*, 5802.
(43) Delmon, D. *Introduction a la Cinetique Heterogene (Introduction to Heterogeneous Kinetics)*; Technip: Paris, France, 1969 (citated by Russian translation: Kinetika Geterogennyh Reakciy, Mir, Moscow, 1972).
(44) Stern, L.; Hogenboom, D. L.; Durham, W. B.; Kirby, S. H.; Chou, I.-M. *J. Phys. Chem. B* **1998**, *102*, 2627.
(45) Istomin, V. A. *Russ. J. Phys. Chem.* **1999**, *73* (11), 1887.
(46) Angell, C. A. *Annu. Rev. Phys. Chem.* **1983**, *34*, 593.
(47) Mel'nikov, V. P.; Nesterov, A. N.; Reshetnikov, A. M. *Dokl. Earth Sci. A* **2003**, *389* (3), 455.
(48) Takeya, K.; Nango, K.; Sugahara, T.; Ohgaki, K.; Tani, A. *J. Phys. Chem. B* **2005**, *109*, 21086.